Theory for the Excitation Spectrum of High-T_c Superconductors: Quasiparticle Dispersion and Shadows of the Fermi Surface

M. Langer, J. Schmalian, S. Grabowski, and K. H. Bennemann
Institut für Theoretische Physik, Freie Universität Berlin, Arnimallee 14, 14195 Berlin, Germany
(Received 15 May 1995)

Using a new method for the solution of the fluctuation exchange approximation equations, which allows the determination of the self-energy $\Sigma_{\mathbf{k}}(\omega)$ of the 2D one-band Hubbard model on the real frequency axis, we calculate the doping dependence of the quasiparticle excitations of high-T_c superconductors. We obtain new results for the shadows of the Fermi surface, their dependence on the deformation of the quasiparticle dispersion, an anomalous ω dependence of $\mathrm{Im}\Sigma_{\mathbf{k}}(\omega)$, and a related violation of the Luttinger theorem. This sheds new light on the influence of short range magnetic order on the low energy excitations and its significance for photoemission experiments.

PACS numbers: 74.25.Jb, 71.27.+a, 79.60.–i

Despite enormous progress, the electronic excitation spectrum of the high-T_c superconductors is still far from being understood [1]. The opening of a spin density gap, the variation in spectral weight as function of momentum $\mathbf{k}$ [2], and the pronounced deformations of the quasiparticle dispersion found by recent angular resolved photoemission experiments [2–6] reflect the strong influence of the electronic correlations on the low energy excitations. Here, the observation of shadows of the Fermi surface (FS) for $Bi_2Sr_2CaCu_2O_{8+\delta}$ [5] by Aebi *et al.* and their relation to short range antiferromagnetic fluctuations in the cuprates is currently most intensively debated [7,8].

The occurrence of shadow states for a system without long range antiferromagnetic order was originally proposed by Kampf and Schrieffer [9]. Using a phenomenological *ansatz* for the spin susceptibility, they argued that for sufficient strong antiferromagnetic correlations a coupling of states $\mathbf{k}$ and $\mathbf{k}'$ with $|\mathbf{k}' - \mathbf{k} - \mathbf{Q}| < \xi^{-1}$ and $\mathbf{Q} = (\pi, \pi)$ might lead to distinct shadow states in photoemission experiments. From their calculation one can estimate that the magnetic correlation length ξ has to be approximately 20 lattice spacings to obtain observable satellite peaks. This is much larger than the correlation length deduced from neutron scattering experiments [10], which is of the order of a few lattice spacings. Therefore, it was stated in Ref. [7] that the observations of Aebi *et al.* cannot be of antiferromagnetic origin.

In this Letter we present the quasiparticle excitation spectrum of the one-band Hubbard model in the normal state using a new numerical method for the self-consistent solution of the fluctuation exchange approximation (FLEX) [11,12] on the real frequency axis. For the first time, we obtain the low energy shadow states and simultaneously a small correlation length ξ. Furthermore, we find deformations of the dispersion at the wave vector $\mathbf{k} = (\pi, 0)$ upon doping, an unusual momentum and frequency dependence of the self-energy, and a violation of the Luttinger theorem as a function of doping.

Since we expect spin fluctuations to be the dominating low energy excitations in the doping region between simple metallic and antiferromagnetic behavior, we use in the following the FLEX approximation to investigate the short range antiferromagnetic order in the cuprates. This perturbative low energy approach is complementary to the exact diagonalization (ED) [13] or quantum Monte Carlo (QMC) studies [14,15], which gave deep insight into the origin of the quasiparticles of strongly correlated materials, but are limited to small finite systems.

In the FLEX approximation the self-energy $\Sigma(\mathbf{k}, i\omega_n)$ of the paramagnetic phase is related to an effective interaction $V(\mathbf{q}, i\omega_n)$ resulting from the self-consistent summation of electron-hole ladder and bubble diagrams within the finite temperature Matsubara formalism for fermionic frequencies ω_n [16]. In general the FLEX equations are solved on the imaginary frequency axis, because of the simple mathematical structure of the Green's functions and the straightforward applicability of the numerically very effective fast Fourier transformation (FFT). Unfortunately, reliable information about the interesting dynamical excitation spectrum that is given on the real frequency axis can only be obtained by analytical continuation of the self-energy $\Sigma(\mathbf{k}, i\omega_n)$ or the electronic Green's function $G(\mathbf{k}, i\omega_n)$. This bears enormous numerical problems and smears out important fine structures. Therefore, we developed a new numerical method for the direct calculation of the electronic self-energy $\Sigma(\mathbf{k}, \omega + i0^+)$ on the real axis [17]. Our approach treats the FLEX equations self-consistently for complex frequencies $z = \omega + i\gamma$ with small but finite imaginary part $\gamma < \pi T$, where T is the temperature. Then, the analytical continuation to the real axis $\gamma \rightarrow 0^+$ is numerically well defined. We strongly believe that without our highly accurate algorithm the new physical results presented below could not have been obtained [18].

In the following, we apply our approach to the one-band Hubbard Hamiltonian that is the minimal model for the CuO_2 planes. The bare dispersion is given by $\varepsilon^0_{\mathbf{k}} = -2t[\cos(k_x) + \cos(k_y)] - \mu$ with nearest neighbor hopping element $t = 0.25$ eV and chemical potential μ. The local Coulomb repulsion is $U = 4t$ [12,19]. The actual calculations presented in this paper are performed

 0031-9007/95/75(24)/4508(4)$06.00

on a (64×64) square lattice in momentum space by using 4096 equally spaced energy points in the interval $[-30t, 30t]$ leading to a low energy resolution of $0.014t \approx 4$ meV.

In the inset of Fig. 1, we show results for the density of states $\varrho(\omega)$ for various doping values $x = 1 - n$ and $T = 63$ K. Here, n is the occupation number per site. We find for larger doping a rigid bandlike behavior, but for smaller doping a pseudogap is visible as a precursor of the spin density wave gap. From the asymmetry with respect to the pseudogap, a transfer of spectral weight from high energy to low energy scales [20] can be seen. To check the influence of finite size effects we compared our data with results obtained from systems with different lattice sizes. For a (32×32) lattice the pseudogap gets considerably smaller, whereas for a (128×128) system it becomes slightly larger. Our finite size analyses showed that all physical conclusions of this paper and, in particular, the shadow states are not influenced by finite size effects. In addition, we find that our results are not sensitively dependent on the temperature in the region of interest, because the characteristic energy scales are of the order of 700 K.

In Fig. 1, we show the momentum resolved spectral density $A(\mathbf{k}, \omega) = -\frac{1}{\pi} \operatorname{Im} G(\mathbf{k}, \omega)$ for $\mathbf{k}$ points between the $(\pi, 0)$ and (π, π) point for $x = 0.12$. The $\mathbf{k}$ point $(\pi, \pi/8)$ is shifted by $\mathbf{Q}$ with respect to the main FS, where one would expect the shadows of the FS induced by antiferromagnetic correlations. Indeed, besides the main peak above the Fermi energy at $\omega = 0$ small satellite peaks can clearly be observed below the Fermi level. Furthermore, the satellite of the spectral density at $\mathbf{k} = (\pi, \pi/8)$ is closest to the Fermi energy, where it merges with the main band. Note that these satellites approach the Fermi level up to $\omega \approx 20$ meV and consequently can be detected in a fixed energy scan of the Brillouin zone with energy width of the order of $\Delta\omega \approx 30$ meV as in the experiment [5]. The intensity of the shadow states of these $\mathbf{k}$ points roughly agrees with Ref. [5]. The width of the shadow structure in $\mathbf{k}$ space, estimated by considering the number of $\mathbf{k}$ points whose satellites contribute significantly to the spectral density, was found to be $\Delta k \approx \pi/5$. This is in good agreement with the experimental result $\Delta k_{\mathrm{exp}} \approx \pi/4$. Most interestingly and in distinction to the phenomenological predictions by Kampf and Schrieffer we obtain a magnetic correlation length $\xi = 2.5$ lattice spacings, which is in very good agreement with neutron scattering experiments [10]. Here, we calculated ξ from the $\mathbf{k}$ dependence of the spin susceptibility by neglecting vertex corrections of the irreducible particle hole bubble. Recently it was discussed [19] that this is a reasonable approximation that slightly overestimates the magnitude of the spin susceptibility.

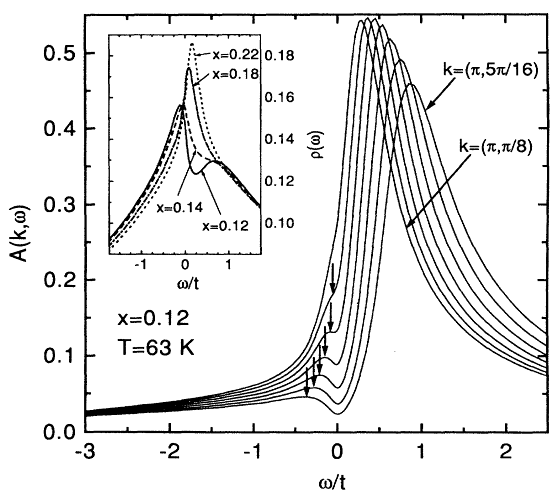

FIG. 1. Spectral density for $\mathbf{k}$ points between the $(\pi, 0)$ and (π, π) point, i.e., $\mathbf{k} = (\pi, \frac{l}{32}\pi)$ with $l = 4, \ldots, 10$. The small satellites, indicated by the arrows, are the shadows of the Fermi surface. The inset shows the density of states $\varrho(\omega)$ for various doping values and $T = 63$ K.

In order to investigate the interdependence of shadow bands and antiferromagnetic correlations, we show in Fig. 2 results for the quasiparticle dispersion obtained from the maxima of the spectral density in the neighborhood of the $(\pi, 0)$ point. For larger doping (dashed line), the saddle point, responsible for the Van Hove singularity, is visible. However, for smaller doping (solid and open squares) pronounced deformations of the dispersion occur. The dispersion of the states with high spectral weight (solid squares) is flattened at an energy $\omega \approx 25$ meV slightly above the Fermi energy and is suddenly repelled from this energy. This is a precursor of the large spin density gap at the $(\pi, 0)$ point. However, the range in $\mathbf{k}$ space where the bands are flat is slightly smaller compared to ED calculations [13] and observed experimentally in $Bi_2Sr_2CaCu_2O_{8+\delta}$ [21]. Furthermore, new quasiparticle

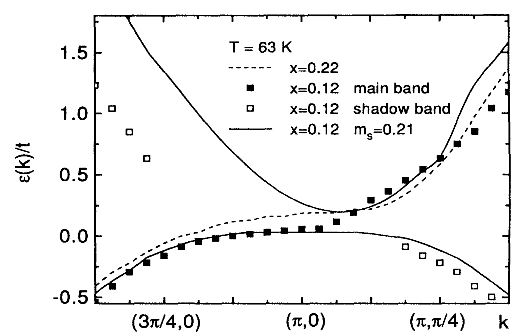

FIG. 2. Quasiparticle dispersion in the neighborhood of the $(\pi, 0)$ point for different doping concentrations. For smaller doping ($x = 0.12$) two bands exist near the Fermi energy. The dispersion of the main band (solid squares) is similar to the highly doped system (dashed line). Considering both, the main band and the shadow band (open squares), one recognizes the evolution towards the two branches of the dispersion in an antiferromagnetic background (solid lines).

states with low spectral weight (open squares) can be observed in Fig. 2. These states, which are visible for larger doping only far away from the Fermi level (not shown), exist for low excitation energies and form the shadows of the FS, but never cross the Fermi level. The magnetic origin of the dispersion can also be supported by performing a spin resolved FLEX approximation with a given antiferromagnetically ordered magnetic moment of $m_s = 0.21$ (which is the Hartree-Fock value). The resulting dispersion (solid line) is a continuation of the situation in the paramagnetic phase for low doping. Therefore the shadow states are a precursor of the antiferromagnetic state for finite but very low excitation energies and are present in a system without long range antiferromagnetic order.

In distinction to the idea of Kampf and Schrieffer [9], the satellites of our calculation are not produced by new poles of the Green's function, but purely by quasiparticle decay processes due to the strong coupling of states with momentum $\mathbf{k}$ at the FS and states $\mathbf{k} + \mathbf{Q}$ at its shadow. In order to demonstrate the effects of this coupling for states close to the Fermi energy we show in Fig. 3 $\mathrm{Im}\Sigma_{\mathbf{k}}(\omega = 0)$ for the doping concentrations $x = 0.16$ and $x = 0.12$. For even larger doping (not shown) this quantity is found to be maximal for states at the FS. For intermediate doping ($x = 0.16$), $\mathrm{Im}\Sigma_{\mathbf{k}}(\omega = 0)$ is strongly enhanced on the FS and more interestingly on its shadow. Nevertheless, no shadow states in $A(\mathbf{k}, \omega)$ are observable for this doping concentration. For small doping ($x = 0.12$), $\mathrm{Im}\Sigma_{\mathbf{k}}(\omega = 0)$ is dominated by the contributions of the shadow states. The enhancement of the low energy scattering rate for *all* $\mathbf{k}$ points shifted by $\mathbf{Q}$ relative to the main FS leads to satellite peaks as in Fig. 1 on the whole shadow of the FS. These effects are in our calculation mostly pronounced for $\mathbf{k} = (\pi, \pi/8)$, whereas on the diagonal the intensity of the shadow states is much weaker, but clearly visible.

The intensity of a shadow peak at $\mathbf{k} + \mathbf{Q}$ is higher the larger the antiferromagnetic correlation length as already discussed by Kampf and Schrieffer [9]. However, this intensity is also determined by the amount of states $\mathbf{k}'$ around $\mathbf{k}$, which are coupled to $\mathbf{k} + \mathbf{Q}$ by antiferromagnetic spin fluctuations. Here, only states $\mathbf{k}'$ with energies $\epsilon_{\mathbf{k}'}$ close to the Fermi level can participate in the formation of a shadow at $\mathbf{k} + \mathbf{Q}$. Since the correlation length was found to be small, it is necessary to have large effective masses to form a shadow state. Consequently, the shadow states are strongly dependent on the deformation of the dispersion due to the electronic correlations. Hence, the existence of flat bands explains our results that the shadow peak is largest near $(\pi, \pi/8)$.

Although we believe that our model dispersion captures the important physical mechanism of the shadow band phenomenon, an improved agreement with the experiments requires an improvement of the quasiparticle dispersion near $(\pi/2, \pi/2)$ and a more realistic description of the topology of the FS [4]. This might be achieved by taking into account next nearest neighbor and other hopping elements [22].

A further interesting consequence of the occurrence of shadow states is the nonconservation of the volume n_{Lutt} inside the FS for small doping. In Fig. 4, results are shown for the FS for different band fillings in comparison with that for $U = 0$. The FS is obtained from the $\mathbf{k}$ points, where $\varepsilon_{\mathbf{k}}^0 + \mathrm{Re}\Sigma_{\mathbf{k}}(0) = 0$. The changes of the FS are rather small, but a tendency towards an enhanced nesting is clearly visible. For larger doping, the Luttinger theorem (LT) is fulfilled. However, for smaller doping the volume of the FS decreases compared to the $U = 0$ case. Calculating n_{Lutt} for different doping we get $n_{\mathrm{Lutt}} = 0.800 = n$ for $x = 0.20$ and $n_{\mathrm{Lutt}} = 0.869 < n$ for $x = 0.12$. This violation of the LT [23] results physically from a transfer of particles to the additional shadow states outside the main FS. Note that this result is no artifact of the FLEX approximation itself. Since this diagrammatic approach is

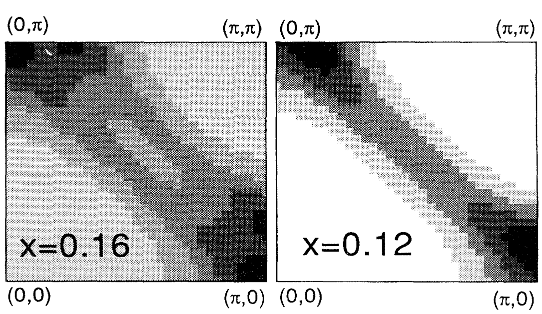

FIG. 3. $\mathrm{Im}\Sigma_{\mathbf{k}}(\omega = 0)$ for two doping concentrations in the first quadrant of the Brillouin zone in a linear grey scale, where dark regions correspond to large decay rates. The intensities for each plot are normalized by its maximum value.

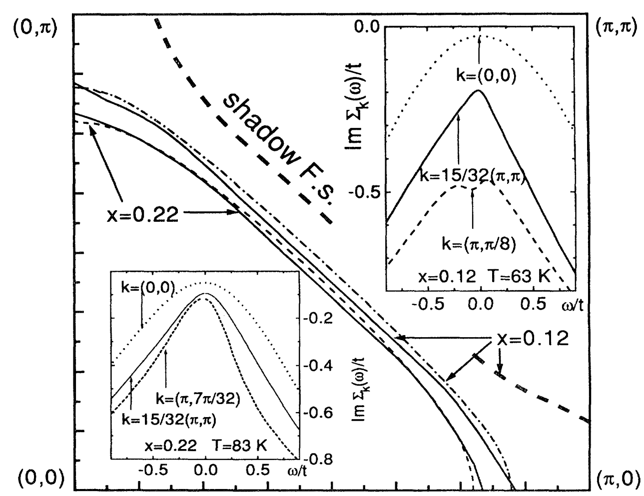

FIG. 4. Fermi surface in the first quadrant of the Brillouin zone in comparison with that of the uncorrelated system for two different doping concentrations. The dashed (solid) lines correspond to $U = 0$ ($U = 4t$). The insets show the frequency dependence of $\mathrm{Im}\Sigma_{\mathbf{k}}(\omega)$ for different doping values. For $x = 0.12$ the shadow of the FS is shown.

conserving in the sense of Baym and Kadanoff, the validity of the LT depends purely on the frequency behavior of the imaginary part of the self-energy [24]. In the insets of Fig. 4, we show $\mathrm{Im}\Sigma_{\mathbf{k}}(\omega)$ for various **k** points. For small doping, our results exhibit a very anomalous **k** and ω dependence as can be seen in the upper right inset of Fig. 4. At the FS, the transition from a low frequency ω^2 to a linear in ω behavior occurs below 5 meV. Moreover, at $\mathbf{k} = (\pi, \pi/8)$, where the shadow band approaches the Fermi level, we find a double well structure reflecting the strong coupling of the shadow states to the main FS as precursor of the singular behavior of $\mathrm{Im}\Sigma_{\mathbf{k}}(\omega)$ in the antiferromagnetic state [9]. This anomalous frequency dependence violates the LT, and the volume of the FS decreases as shown in Fig. 4. A first experimental indication for this phenomenon was recently found by Liu *et al.* [3]. For larger doping, our theory yields the conventional Fermi-liquid behavior $\mathrm{Im}\Sigma_{\mathbf{k}}(\omega) \propto (\omega^2 + cT^2)$, where c is a constant. A clear demonstration of this trend is given in the lower left inset of Fig. 4. Here, $\mathrm{Im}\Sigma_{\mathbf{k}}(\omega)$ is considerably smaller for $\omega = 0$, much less **k** dependent and proportional to ω^2 up to much higher frequencies. Consequently no violation of the LT can be observed.

In conclusion, using a new method for the solution of the FLEX equations on the real frequency axis, we investigated the fine structure of the excitation spectrum for high-T_c superconductors in the framework of the one-band Hubbard model. We obtained for the first time within a microscopic approach using a model dispersion shadows of the FS without long range antiferromagnetic order. These shadow states are induced by dynamical spin fluctuations and are due to the fact that for **k** points above the Fermi momentum spectral weight is transferred below the Fermi energy as a precursor effect of the oncoming antiferromagnetic phase transition. In addition, these shadows occur for small excitation energies in agreement with the experiments by Aebi *et al.* [5]. All this shows clearly that the quasiparticle properties of the cuprates are closely intertwined with the strong but short ranged antiferromagnetic correlations [25]. In a forthcoming publication, we use our method to discuss the development of the shadow states below T_c and their significance for photoemission experiments [26].

We acknowledge the financial support of the BMFT and the DFG and are grateful for valuable discussions with P. Aebi.

Note added.—After submission of the present Letter, Haas, Moreo, and Dagotto [27] published a work investigating antiferromagnetically induced photoemission bands by using QMC and ED techniques. Similar to our study they observed transfer of spectral weight below the Fermi energy. However, they were not able to detect the shadows of the Fermi surface within the experimental energy width due to their limited resolution in momentum space.

[1] E. Dagotto, Rev. Mod. Phys. **66**, 763 (1994), and references therein.
[2] B. O. Wells *et al.,* Phys. Rev. Lett. **74**, 964 (1995).
[3] R. Liu *et al.,* Phys. Rev. B **46**, 11 056 (1992).
[4] Z. X. Shen and D. S. Dessau, Phys. Rep. **253**, 1 (1995).
[5] P. Aebi *et al.,* Phys. Rev. Lett. **72**, 2757 (1994).
[6] K. Gofron *et al.,* Phys. Rev. Lett. **73**, 3302 (1994).
[7] S. Chakravarty, Phys. Rev. Lett. **74**, 1885 (1995).
[8] P. Aebi *et al.,* Phys. Rev. Lett. **74**, 1886 (1995).
[9] A. P. Kampf and J. R. Schrieffer, Phys. Rev. B **42**, 7967 (1990).
[10] J. M. Tranquada *et al.,* Phys. Rev. B **46**, 5561 (1992).
[11] N. E. Bickers and D. J. Scalapino, Ann. Phys. (N.Y.) **193**, 206 (1989).
[12] N. E. Bickers, D. J. Scalapino, and S. R. White, Phys. Rev. Lett. **62**, 961 (1989).
[13] E. Dagotto, A. Nazarenko, and M. Bonisengi, Phys. Rev. Lett. **73**, 728 (1994).
[14] N. Bulut, D. J. Scalapino, and S. R. White, Phys. Rev. Lett. **72**, 705 (1994).
[15] R. Preuss, W. Hanke, and W. von der Linden, Phys. Rev. Lett. **75**, 1344 (1995).
[16] Note that we neglect the contributions of the particle-particle excitations, which were shown to be of minor importance in Ref. [12].
[17] Details will be published elsewhere.
[18] The main advantage of our method compared to the first real frequency approach recently published by Dahm and Tewordt [19] is the subsequent use of the FFT for momentum and frequency space and the consistent solution for a small but finite imaginary part γ. This leads to a numerical very stable method limiting the deviations in the spectral density from loop to loop per momentum and frequency point to 10^{-5}.
[19] T. Dahm and L. Tewordt, Phys. Rev. Lett. **74**, 793 (1995); Phys. Rev. B **52**, 1297 (1995).
[20] H. Eskes *et al.,* Phys. Rev. Lett. **67**, 1035 (1991).
[21] Our dispersion is in better agreement with the single layer system $Bi_2Sr_2CuO_{6+\delta}$ [4]. Therefore, it is unclear if the discrepancy between our dispersion and that in $Bi_2Sr_2CaCu_2O_{8+\delta}$ is due to a weakness of FLEX or to interlayer effects.
[22] The two important prerequisites for shadow states contained in our model, namely, flat quasiparticle dispersion and FS nesting, were observed in various cuprate systems [4] and are also a basic content of more realistic parametrizations of band structure calculations; see also O. K. Andersen *et al.,* Phys. Rev. B **49**, 4145 (1994).
[23] J. M. Luttinger, Phys. Rev. **119**, 1153 (1961). Note that our calculation refers to finite temperature.
[24] G. Baym and L. P. Kadanoff, Phys. Rev. **124**, 287 (1961); G. Baym, *ibid.* **127**, 1391 (1962).
[25] This means that the effective coupling $V(\mathbf{q}, \omega)$ is large for $\mathbf{q} = \mathbf{Q}$ and of short range.
[26] S. Grabowski, J. Schmalian, M. Langer, and K.-H. Bennemann (to be published).
[27] S. Haas, A. Moreo, and E. Dagotto, Phys. Rev. Lett. **74**, 4281 (1995).

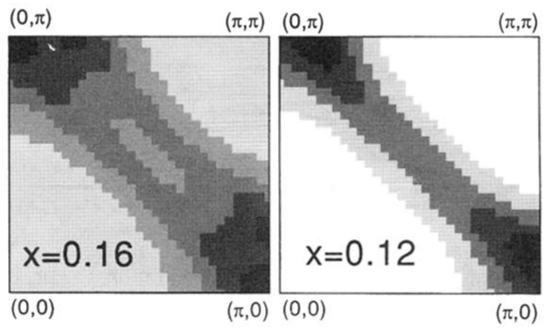

FIG. 3. $\mathrm{Im}\Sigma_{\mathbf{k}}(\omega = 0)$ for two doping concentrations in the first quadrant of the Brillouin zone in a linear grey scale, where dark regions correspond to large decay rates. The intensities for each plot are normalized by its maximum value.